San Andreas Fault Characterization at the LADWP Elizabeth Tunnel

Scott Lindvall[1], Scott Kerwin[2], James Evans[3], Jeffrey Tyson[4], James Chestnut[4], Chris Heron[4], Kevin Mass[4], Kate Scharer[5], Devin McPhillips[5], Diane Moore[5], Michael Farr[2], Christopher Ballard[3], Randolph Williams[6], Kelly Bradbury[3], Christie Rowe[7], and Heather Savage[8]

1) Lettis Consultants International, Inc., 2) Amec Foster Wheeler, 3) Utah State University, 4) Los Angeles Department of Water and Power, 5) US Geological Survey, 6) University of Wisconsin-Madison, 7) McGill University, 8) Lamont Doherty Earth Observatory

Abstract

Newly acquired subsurface data across the San Andreas Fault (SAF) provides insight into the geometry, structure, and composition of the upper part of the SAF zone in the northern Sierra Pelona Mountains, CA. The purpose of the investigation was to characterize the Los Angeles Aqueduct crossing of the SAF in the Elizabeth Tunnel, an 8-km-long tunnel section of the aqueduct that delivers water from Owens Valley to the City of Los Angeles. Several transects of CPT soundings and geotechnical boreholes define a 40-m-thick section of unconsolidated Holocene and Pleistocene alluvial deposits above a faulted and deformed buried bedrock surface. Some of the abrupt separations in the buried bedrock surface correlate with scarps and tonal lineaments observed at the ground surface in historical air photos and lidar. Seven 55°- 65° northeast plunging boreholes acquired a total of ~ 750 m of rock core to a maximum vertical depth of 140 m, across the ~150 m wide fault zone. Core recovery was ~95%, and the core samples consist of a range of indurated fault-related rocks including zones of foliated cataclasite and a few local intervals of clay-rich gouge. The cataclasite zones have an estimated local thickness up to 2 - 3 m and are developed within granodiorite to granitoid gneiss. Outside of the primary cataclasite/gouge zones, the damage zones are defined by more discrete deformation such as cataclastic shear bands. In most cases, cataclasite and gouge zones correlate with prominent resistivity lows observed in wireline logs. A tentative correlation of slip surfaces observed across the boreholes indicates that the principal fault surfaces dip steeply south, flower and flatten near the upper parts of the holes, and may connect to the active surface traces of the SAF as interpreted from the offset buried bedrock surface and topography. Fault-related rocks throughout the boreholes exhibit evidence for fluid-fault interactions in the form of variably developed clay-rich shear bands/zones and hydrothermal alteration products. The degree of induration and alteration indicate that the fault zone here consists of numerous slip surfaces in a hydrothermally altered and “cemented” sequence. Future analyses of core samples will provide insight into the combined mechanical and chemical processes responsible for fault-zone development in this upper part of the SAF, with a particular focus on how these processes operate throughout the seismic cycle.

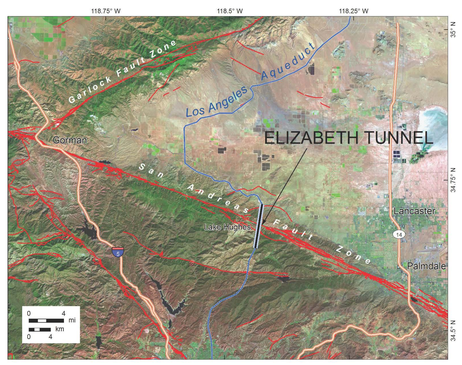

Figure 1. Location map of the Elizabeth Tunnel crossing of the San Andreas fault. The tunnel is part of the Los Angeles Aqueduct (LAA) system operated by the Los Angeles Department of water and Power (LADWP).

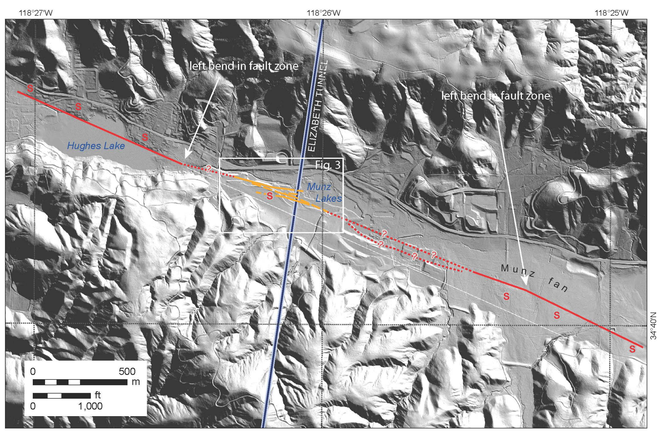

Figure 2. Local changes in fault strike near Elizabeth Tunnel. Three scarps (s) along the northern margin of Hughes Lake define a strike of ~N65W, which changes to ~N75W as it approaches the tunnel. The fault is not well expressed in the ground surface between the tunnel and scarps in Munz fan where dashed and querried. Local faults defined in subsurface by CPT and boring transects shown in orange. Base image is hillshade from 2015 LiDAR. Orientation of the fault zone at the tunnel is more westerly than regional strike, implying local trasnspression.

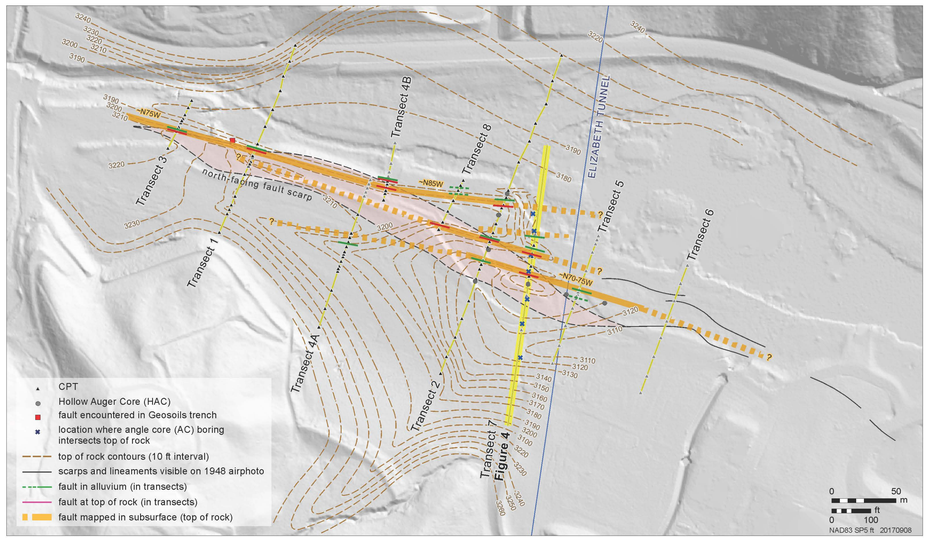

Figure 3. Map of the Elizabeth Tunnel crossing showing CPT and boring transects, surficial fault scarps and lineaments, contours on buried bedrock surface, and faults mapped based on vertical separation of the buried bedrock surface. Base map is hillshade from LiDAR acquired in 2015.

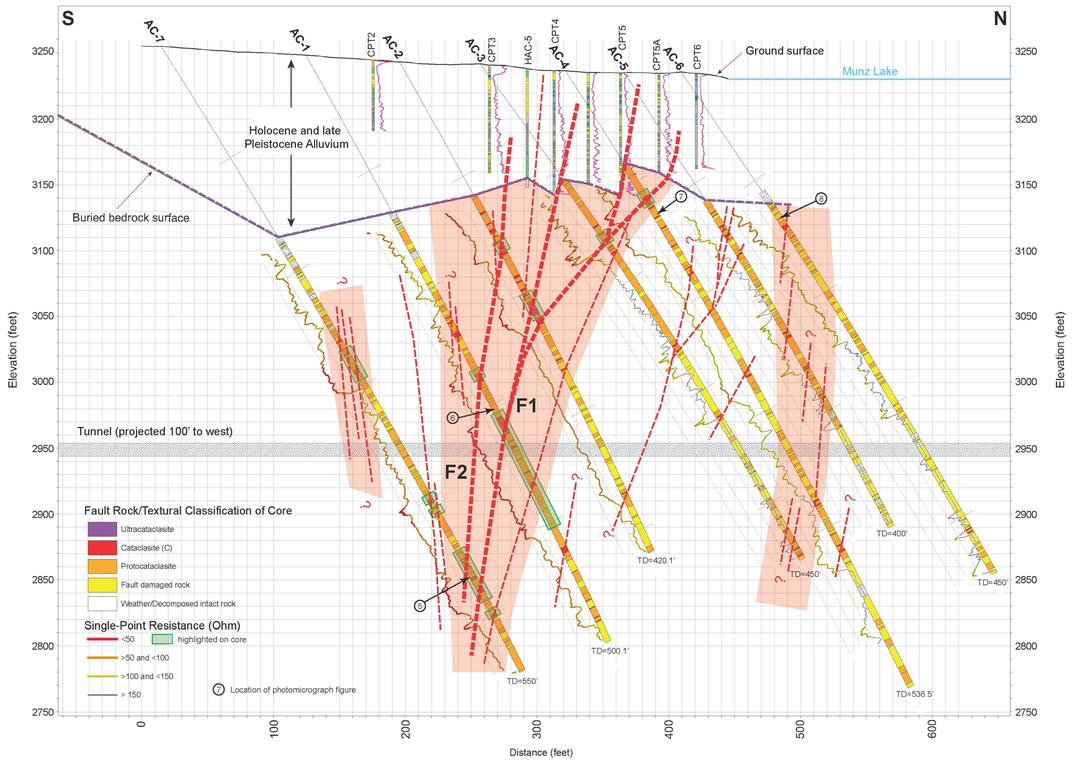

Figure 4. Cross section along Transect 7 illustrating interpreted fault zone geometry. Thick red lines denote most prominant zones of cataclasite and ultracataclasite, which are interpreted to represent the primary fault strands (F1 and F2) with the most cumulative slip. Thin red lines represent thinner and less prominant faults. Light red shading highlights areas of concentrated deformation with more abundant cataclasite intervals. Given the uncertainty in orientations of faults encountered in core, this is not a unique solution and correlation of individual cataclasites from boring to boring is somewhat speculative. This interpretation of the fault zone shown in this figure assumes a transpressive environment and flowering structure, which is consistent with the geometry of fault F1 and the local strike of the fault zone. Fault rock textures classified in the cores are based on visual inspection core and over 50 thin section petrographic analyses. Curves of single-point resistance, which was the most diagnostic down-hole geophysical measurement for identifying intervals of cataclasite, are shown for each angle core boring. The intervals of lowest resistivity (< 50 Ohms) are indicated by green shading on core borings.

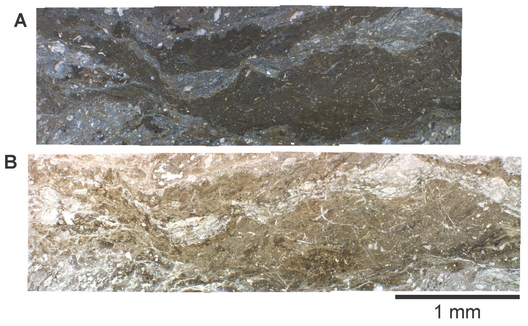

Figure 5. Photomicrograph of ultracataclasite from near fault F1 in AC-7 core at 467 ft depth. **A** - Cross polarized light; **B** - Plane of polarized light images of very fine-grained, strongly foliated rocks.

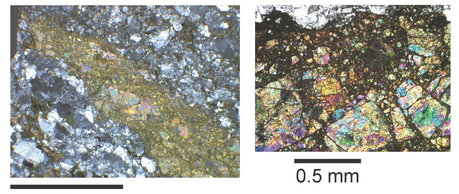

Figure 6. Photomicrographs of epidote-filled zone exhibiting cataclasis in AC-1 core at 305 ft depth. Epidote is typically of hydrothermal origin in these settings (>100° C), and the relationships here indicate hydrothermal fluid flow was followed by brittle deformation along the mineralized zone.

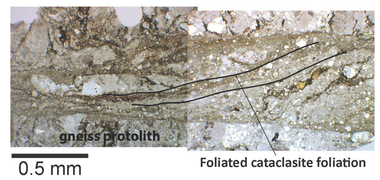

Figure 7. Photomicrograph of well-developed foliated cataclasite below fault F1 in AC-4 at 130 ft depth. Gneissic protolith on either side with sharp boundary of a fault comprised of highly comminuted quartz and feldspar, and a fine-grained Fe-oxides and clays.

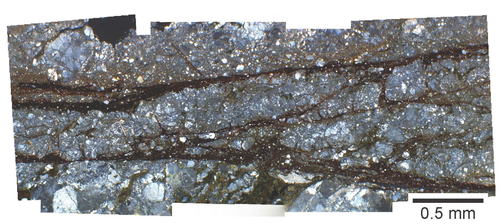

Figure 8. Cross polarized light photomosaic of mulitple narrow Fe-oxide rich slip surfaces in a cataclasite matrix from boring AC-6 at 134 ft depth. Development of Fe-rich zones occured after the development of the cataclasite.

September 2017